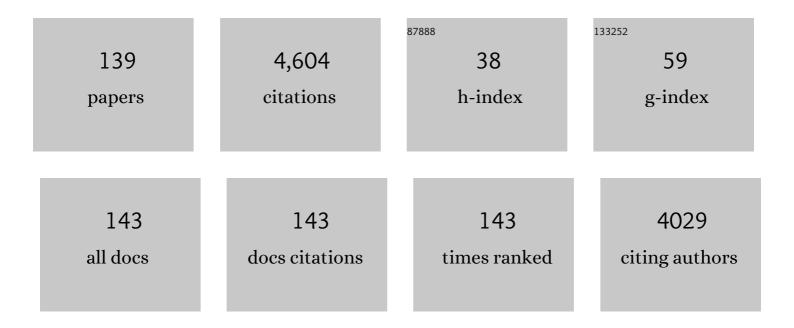
Ulf-Peter Apfel

List of Publications by Year in descending order

Source: https://exaly.com/author-pdf/3150622/publications.pdf Version: 2024-02-01



#	Article	IF	CITATIONS
1	Introducing Waterâ€Networkâ€Assisted Proton Transfer for Boosted Electrocatalytic Hydrogen Evolution with Cobalt Corrole. Angewandte Chemie - International Edition, 2022, 61, e202114310.	13.8	46
2	[NiFe]-(Oxy)Sulfides Derived from NiFe2O4 for the Alkaline Hydrogen Evolution Reaction. Energies, 2022, 15, 543.	3.1	5
3	A bioinspired redox-modulating copper(<scp>ii</scp>)–macrocyclic complex bearing non-steroidal anti-inflammatory drugs with anti-cancer stem cell activity. Dalton Transactions, 2022, 51, 5904-5912.	3.3	12
4	Metal orroleâ€Based Porous Organic Polymers for Electrocatalytic Oxygen Reduction and Evolution Reactions. Angewandte Chemie - International Edition, 2022, 61, .	13.8	54
5	Hidden parameters for electrochemical carbon dioxide reduction in zero-gap electrolyzers. Cell Reports Physical Science, 2022, 3, 100825.	5.6	17
6	Metalâ€Corroleâ€Based Porous Organic Polymers for Electrocatalytic Oxygen Reduction and Evolution Reactions. Angewandte Chemie, 2022, 134, .	2.0	9
7	Electrochemical CO2 reduction toward multicarbon alcohols - The microscopic world of catalysts & process conditions. IScience, 2022, 25, 104010.	4.1	32
8	Electrochemical CO2 reduction - The macroscopic world of electrode design, reactor concepts & amp; economic aspects. IScience, 2022, 25, 104011.	4.1	46
9	Trimetallic Pentlandites (Fe,Co,Ni) ₉ S ₈ for the Electrocatalytical HER in Acidic Media. ACS Materials Au, 2022, 2, 474-481.	6.0	9
10	Tuning the Electronic Properties of Homoleptic Silver(I) bis-BIAN Complexes towards Efficient Electrocatalytic CO2 Reduction. Catalysts, 2022, 12, 545.	3.5	6
11	Bioinspired iron porphyrins with appended poly-pyridine/amine units for boosted electrocatalytic CO2 reduction reaction. EScience, 2022, 2, 623-631.	41.6	23
12	Trapping an Oxidized and Protonated Intermediate of the [FeFe]-Hydrogenase Cofactor under Mildly Reducing Conditions. Inorganic Chemistry, 2022, 61, 10036-10042.	4.0	5
13	Role‧pecialized Division of Labor in CO ₂ Reduction with Doublyâ€Functionalized Iron Porphyrin Atropisomers. Angewandte Chemie - International Edition, 2022, 61, .	13.8	23
14	Electrochemical CO ₂ Reduction: Tailoring Catalyst Layers in Gas Diffusion Electrodes. Advanced Sustainable Systems, 2021, 5, 2000088.	5.3	50
15	Mesoporous NiFe ₂ O ₄ with Tunable Pore Morphology for Electrocatalytic Water Oxidation. ChemElectroChem, 2021, 8, 227-239.	3.4	15
16	A bioinspired oxoiron(<scp>iv</scp>) motif supported on a N ₂ S ₂ macrocyclic ligand. Chemical Communications, 2021, 57, 2947-2950.	4.1	11
17	Site-selective protonation of the one-electron reduced cofactor in [FeFe]-hydrogenase. Dalton Transactions, 2021, 50, 3641-3650.	3.3	13
18	[FeFe]-Hydrogenases: maturation and reactivity of enzymatic systems and overview of biomimetic models. Chemical Society Reviews, 2021, 50, 1668-1784.	38.1	136

#	Article	IF	CITATIONS
19	A dithiacyclam-coordinated silver(<scp>i</scp>) polymer with anti-cancer stem cell activity. Dalton Transactions, 2021, 50, 5779-5783.	3.3	7
20	A safety cap protects hydrogenase from oxygen attack. Nature Communications, 2021, 12, 756.	12.8	42
21	Investigation of Cyclam Based Reâ€Complexes as Potential Electrocatalysts for the CO ₂ Reduction Reaction. Zeitschrift Fur Anorganische Und Allgemeine Chemie, 2021, 647, 968-977.	1.2	6
22	Controlling Oxygen Reduction Selectivity through Steric Effects: Electrocatalytic Twoâ€Electron and Fourâ€Electron Oxygen Reduction with Cobalt Porphyrin Atropisomers. Angewandte Chemie - International Edition, 2021, 60, 12742-12746.	13.8	85
23	Crossing the Valley of Death: From Fundamental to Applied Research in Electrolysis. Jacs Au, 2021, 1, 527-535.	7.9	79
24	Synergistic Electrocatalytic Hydrogen Evolution in Ni/NiS Nanoparticles Wrapped in Multi-Heteroatom-Doped Reduced Graphene Oxide Nanosheets. ACS Applied Materials & Interfaces, 2021, 13, 34043-34052.	8.0	33
25	Magnetic NiFe ₂ O ₄ Nanoparticles Prepared via Nonâ€Aqueous Microwaveâ€Assisted Synthesis for Application in Electrocatalytic Water Oxidation. Chemistry - A European Journal, 2021, 27, 16990-17001.	3.3	21
26	Promising Membrane for Polymer Electrolyte Fuel Cells Shows Remarkable Proton Conduction over Wide Temperature and Humidity Ranges. ACS Applied Polymer Materials, 2021, 3, 4275-4286.	4.4	8
27	Fe/Co and Ni/Co-pentlandite type electrocatalysts for the hydrogen evolution reaction. Chinese Journal of Catalysis, 2021, 42, 1360-1369.	14.0	33
28	An asymmetric cryptand for the site-specific coordination of 3d metals in multiple oxidation states. Dalton Transactions, 2021, 50, 14602-14610.	3.3	2
29	Toward electrocatalytic chemoenzymatic hydrogen evolution and beyond. Cell Reports Physical Science, 2021, 2, 100626.	5.6	1
30	Assessing the Influence of Supercritical Carbon Dioxide on the Electrochemical Reduction to Formic Acid Using Carbon-Supported Copper Catalysts. ACS Catalysis, 2020, 10, 12783-12789.	11.2	22
31	The effect of flue gas contaminants on the CO2 electroreduction to formic acid. Journal of CO2 Utilization, 2020, 42, 101315.	6.8	29
32	Plasmachemical Traceâ€Oxygen Removal in a Coke Oven Gas with a Coaxial Packedâ€Bedâ€ĐBD Reactor. Chemie-Ingenieur-Technik, 2020, 92, 1559-1566.	0.8	2
33	Interplay of Spin Crossover and Coordination-Induced Spin State Switch for Iron Bis(pyrazolyl)methanes in Solution. Inorganic Chemistry, 2020, 59, 15343-15354.	4.0	9
34	Frontispiz: Electrocatalytic Reduction of CO ₂ to Acetic Acid by a Molecular Manganese Corrole Complex. Angewandte Chemie, 2020, 132, .	2.0	1
35	Electrochemical CO 2 and Proton Reduction by a Co(dithiacyclam) Complex. Zeitschrift Fur Anorganische Und Allgemeine Chemie, 2020, 646, 746-753.	1.2	9
36	Sustainable and rapid preparation of nanosized Fe/Ni-pentlandite particles by mechanochemistry. Chemical Science, 2020, 11, 12835-12842.	7.4	29

#	Article	IF	CITATIONS
37	Dual-Heteroatom-Doped Reduced Graphene Oxide Sheets Conjoined CoNi-Based Carbide and Sulfide Nanoparticles for Efficient Oxygen Evolution Reaction. ACS Applied Materials & Interfaces, 2020, 12, 40186-40193.	8.0	25
38	Tailoring the Size, Inversion Parameter, and Absorption of Phase-Pure Magnetic MgFe ₂ O ₄ Nanoparticles for Photocatalytic Degradations. ACS Applied Nano Materials, 2020, 3, 11587-11599.	5.0	27
39	Enhancing the CO ₂ Electroreduction of Fe/Niâ€Pentlandite Catalysts by S/Se Exchange. Chemistry - A European Journal, 2020, 26, 9938-9944.	3.3	21
40	Waterâ€Soluble Polymers with Appending Porphyrins as Bioinspired Catalysts for the Hydrogen Evolution Reaction. Angewandte Chemie - International Edition, 2020, 59, 15844-15848.	13.8	76
41	Metalâ€Rich Chalcogenides as Sustainable Electrocatalysts for Oxygen Evolution and Reduction: State of the Art and Future Perspectives. European Journal of Inorganic Chemistry, 2020, 2020, 2679-2690.	2.0	27
42	Frontispiece: Electrocatalytic Reduction of CO ₂ to Acetic Acid by a Molecular Manganese Corrole Complex. Angewandte Chemie - International Edition, 2020, 59, .	13.8	0
43	New Phosphorous-Based [FeFe]-Hydrogenase Models. Catalysts, 2020, 10, 522.	3.5	6
44	Enantioselective Epoxidation by Flavoprotein Monooxygenases Supported by Organic Solvents. Catalysts, 2020, 10, 568.	3.5	8
45	Powering Artificial Enzymatic Cascades with Electrical Energy. Angewandte Chemie - International Edition, 2020, 59, 10929-10933.	13.8	29
46	Shedding Light on Proton and Electron Dynamics in [FeFe] Hydrogenases. Journal of the American Chemical Society, 2020, 142, 5493-5497.	13.7	38
47	Homolytic versus Heterolytic Hydrogen Evolution Reaction Steered by a Steric Effect. Angewandte Chemie - International Edition, 2020, 59, 8941-8946.	13.8	87
48	Metalâ€Rich Chalcogenides for Electrocatalytic Hydrogen Evolution: Activity of Electrodes and Bulk Materials. ChemElectroChem, 2020, 7, 1514-1527.	3.4	55
49	Electrocatalytic Reduction of CO ₂ to Acetic Acid by a Molecular Manganese Corrole Complex. Angewandte Chemie - International Edition, 2020, 59, 10527-10534.	13.8	95
50	Electrochemical CO ₂ Reduction — The Effect of Chalcogenide Exchange in Ni-Isocyclam Complexes. Organometallics, 2020, 39, 1497-1510.	2.3	13
51	Electrocatalytic Reduction of CO ₂ to Acetic Acid by a Molecular Manganese Corrole Complex. Angewandte Chemie, 2020, 132, 10614-10621.	2.0	37
52	Catalytically Active Iron(IV)oxo Species Based on a Bis(pyridinyl)phenanthrolinylmethane. Israel Journal of Chemistry, 2020, 60, 987-998.	2.3	4
53	A dinuclear porphyrin-macrocycle as efficient catalyst for the hydrogen evolution reaction. Chemical Communications, 2020, 56, 14179-14182.	4.1	18
54	Insights from 125Te and 57Fe nuclear resonance vibrational spectroscopy: a [4Fe–4Te] cluster from two points of view. Chemical Science, 2019, 10, 7535-7541.	7.4	5

#	Article	IF	CITATIONS
55	Loss of Specific Active-Site Iron Atoms in Oxygen-Exposed [FeFe]-Hydrogenase Determined by Detailed X-ray Structure Analyses. Journal of the American Chemical Society, 2019, 141, 17721-17728.	13.7	26
56	Molecular cobalt corrole complex for the heterogeneous electrocatalytic reduction of carbon dioxide. Nature Communications, 2019, 10, 3864.	12.8	112
57	Geometry of the Catalytic Active Site in [FeFe]-Hydrogenase Is Determined by Hydrogen Bonding and Proton Transfer. ACS Catalysis, 2019, 9, 9140-9149.	11.2	30
58	How [FeFe]-Hydrogenase Facilitates Bidirectional Proton Transfer. Journal of the American Chemical Society, 2019, 141, 17394-17403.	13.7	38
59	Fe _x Ni _{9â^'x} S ₈ (<i>x</i> = 3–6) as potential photocatalysts for solar-driven hydrogen production?. Faraday Discussions, 2019, 215, 216-226.	3.2	11
60	Bio-inspired design: bulk iron–nickel sulfide allows for efficient solvent-dependent CO ₂ reduction. Chemical Science, 2019, 10, 1075-1081.	7.4	64
61	Sulfur substitution in a Ni(cyclam) derivative results in lower overpotential for CO2 reduction and enhanced proton reduction. Dalton Transactions, 2019, 48, 5923-5932.	3.3	15
62	Synthetic approaches to artificial photosynthesis: general discussion. Faraday Discussions, 2019, 215, 242-281.	3.2	5
63	Niâ€Metalloid (B, Si, P, As, and Te) Alloys as Water Oxidation Electrocatalysts. Advanced Energy Materials, 2019, 9, 1900796.	19.5	93
64	Seleno-analogues of pentlandites (Fe _{4.5} Ni _{4.5} S _{8â^'Y} Se _Y ,) T_2019, 55, 8792-8795.	j ETQq0 0 (4.1	0 rgBT /Overlo 28
65	Bioinspired reactivity and coordination chemistry. Dalton Transactions, 2019, 48, 5859-5860.	3.3	0
66	Differential Protonation at the Catalytic Six-Iron Cofactor of [FeFe]-Hydrogenases Revealed by ⁵⁷ Fe Nuclear Resonance X-ray Scattering and Quantum Mechanics/Molecular Mechanics Analyses. Inorganic Chemistry, 2019, 58, 4000-4013.	4.0	19
67	Solvent-Controlled CO ₂ Reduction by a Triphos–Iron Hydride Complex. Organometallics, 2019, 38, 289-299.	2.3	17
68	(Invited) From Manipulated Enzymes to Solid State Electrodes –Towards the Reduction of Protons and CO2. ECS Meeting Abstracts, 2019, , .	0.0	0
69	[FeFe]-Hydrogenases: recent developments and future perspectives. Chemical Communications, 2018, 54, 5934-5942.	4.1	111
70	Die lokale OberflÃ e henstruktur und â€zusammensetzung bestimmt die Wasserstoffentwicklung an Eisenâ€Nickelsulfiden. Angewandte Chemie, 2018, 130, 4157-4161.	2.0	10
71	Local Surface Structure and Composition Control the Hydrogen Evolution Reaction on Iron Nickel Sulfides. Angewandte Chemie - International Edition, 2018, 57, 4093-4097.	13.8	104
72	Frontispiece: From Enzymes to Functional Materials—Towards Activation of Small Molecules. Chemistry - A European Journal, 2018, 24, .	3.3	0

#	Article	IF	CITATIONS
73	Protonation/reduction dynamics at the [4Fe–4S] cluster of the hydrogen-forming cofactor in [FeFe]-hydrogenases. Physical Chemistry Chemical Physics, 2018, 20, 3128-3140.	2.8	76
74	Hydrogen and oxygen trapping at the H-cluster of [FeFe]-hydrogenase revealed by site-selective spectroscopy and QM/MM calculations. Biochimica Et Biophysica Acta - Bioenergetics, 2018, 1859, 28-41.	1.0	39
75	Influence of the Fe:Ni Ratio and Reaction Temperature on the Efficiency of (Fe _{<i>x</i>} Ni _{1–<i>x</i>}) ₉ S ₈ Electrocatalysts Applied in the Hydrogen Evolution Reaction. ACS Catalysis, 2018, 8, 987-996.	11.2	134
76	From Enzymes to Functional Materials—Towards Activation of Small Molecules. Chemistry - A European Journal, 2018, 24, 1471-1493.	3.3	55
77	Crystallographic and spectroscopic assignment of the proton transfer pathway in [FeFe]-hydrogenases. Nature Communications, 2018, 9, 4726.	12.8	60
78	Cobalt–metalloid alloys for electrochemical oxidation of 5-hydroxymethylfurfural as an alternative anode reaction in lieu of oxygen evolution during water splitting. Beilstein Journal of Organic Chemistry, 2018, 14, 1436-1445.	2.2	58
79	Spectroscopical Investigations on the Redox Chemistry of [FeFe]-Hydrogenases in the Presence of Carbon Monoxide. Molecules, 2018, 23, 1669.	3.8	9
80	Organometallic Fe–Fe Interactions: Beyond Common Metal–Metal Bonds and Inverse Mixedâ€Valent Charge Transfer. Chemistry - A European Journal, 2017, 23, 1770-1774.	3.3	16
81	Anorganische Chemie 2016: Koordinationschemie und Bioanorganik. Nachrichten Aus Der Chemie, 2017, 65, 245-254.	0.0	0
82	Modulation of the CO ₂ fixation in dinickel azacryptands. Dalton Transactions, 2017, 46, 5680-5688.	3.3	10
83	Redox Induced Configurational Isomerization of Bisphosphine–Tricarbonyliron(I) Complexes and the Difference a Ferrocene Makes. Inorganic Chemistry, 2017, 56, 7501-7511.	4.0	22
84	Carbon/Silicon Exchange at the Apex of Diphos―and Triphosâ€Derived Ligands – More Than Just a Substitute?. European Journal of Inorganic Chemistry, 2017, 2017, 3295-3301.	2.0	5
85	Spontaneous Si–C bond cleavage in (Triphos ^{Si})-nickel complexes. Dalton Transactions, 2017, 46, 907-917.	3.3	16
86	Mobile zinc increases rapidly in the retina after optic nerve injury and regulates ganglion cell survival and optic nerve regeneration. Proceedings of the National Academy of Sciences of the United States of America, 2017, 114, E209-E218.	7.1	111
87	Sunlightâ€Dependent Hydrogen Production by Photosensitizer/Hydrogenase Systems. ChemSusChem, 2017, 10, 894-902.	6.8	44
88	Protonâ€Coupled Reduction of the Catalytic [4Feâ€4S] Cluster in [FeFe]â€Hydrogenases. Angewandte Chemie - International Edition, 2017, 56, 16503-16506.	13.8	56
89	Bridging Hydride at Reduced H-Cluster Species in [FeFe]-Hydrogenases Revealed by Infrared Spectroscopy, Isotope Editing, and Quantum Chemistry. Journal of the American Chemical Society, 2017, 139, 12157-12160.	13.7	53
90	Electronic and molecular structure relations in diiron compounds mimicking the [FeFe]-hydrogenase active site studied by X-ray spectroscopy and quantum chemistry. Dalton Transactions, 2017, 46, 12544-12557.	3.3	8

#	Article	IF	CITATIONS
91	<i>Operando</i> Phonon Studies of the Protonation Mechanism in Highly Active Hydrogen Evolution Reaction Pentlandite Catalysts. Journal of the American Chemical Society, 2017, 139, 14360-14363.	13.7	53
92	Accumulating the hydride state in the catalytic cycle of [FeFe]-hydrogenases. Nature Communications, 2017, 8, 16115.	12.8	93
93	Monodispersed Mesoporous Silica Spheres Supported Co ₃ O ₄ as Robust Catalyst for Oxygen Evolution Reaction. ChemCatChem, 2017, 9, 4238-4243.	3.7	15
94	Spectroscopic and reactivity differences in metal complexes derived from sulfur containing Triphos homologs. Dalton Transactions, 2017, 46, 13251-13262.	3.3	3
95	Simple Methods for the Preparation of Non-noble Metal Bulk-electrodes for Electrocatalytic Applications. Journal of Visualized Experiments, 2017, , .	0.3	3
96	Protonengekoppelte Reduktion des katalytischen [4Feâ€4S]â€Zentrums in [FeFe]â€Hydrogenasen. Angewandte Chemie, 2017, 129, 16728-16732.	2.0	7
97	Interplay between CN [–] Ligands and the Secondary Coordination Sphere of the H-Cluster in [FeFe]-Hydrogenases. Journal of the American Chemical Society, 2017, 139, 18222-18230.	13.7	42
98	Chalcogenide substitution in the [2Fe] cluster of [FeFe]-hydrogenases conserves high enzymatic activity. Dalton Transactions, 2017, 46, 16947-16958.	3.3	48
99	Mechanistic Implications for the Ni(I)-Catalyzed Kumada Cross-Coupling Reaction. Inorganics, 2017, 5, 78.	2.7	25
100	[FeFe]â€Hydrogenase with Chalcogenide Substitutions at the H luster Maintains Full H ₂ Evolution Activity. Angewandte Chemie - International Edition, 2016, 55, 8396-8400.	13.8	53
101	Towards Iron-Catalyzed Sonogashira Cross-Coupling Reactions. ChemistrySelect, 2016, 1, 2717-2721.	1.5	7
102	Stepwise isotope editing of [FeFe]-hydrogenases exposes cofactor dynamics. Proceedings of the National Academy of Sciences of the United States of America, 2016, 113, 8454-8459.	7.1	60
103	Electrochemical Investigations of the Mechanism of Assembly of the Active-Site H-Cluster of [FeFe]-Hydrogenases. Journal of the American Chemical Society, 2016, 138, 15227-15233.	13.7	38
104	Pentlandite rocks as sustainable and stable efficient electrocatalysts for hydrogen generation. Nature Communications, 2016, 7, 12269.	12.8	150
105	[FeFe]â€Hydrogenase with Chalcogenide Substitutions at the H luster Maintains Full H ₂ Evolution Activity. Angewandte Chemie, 2016, 128, 8536-8540.	2.0	15
106	Phosphine-ligated dinitrosyl iron complexes for redox-controlled NO release. Dalton Transactions, 2016, 45, 10271-10279.	3.3	13
107	Koordinationschemie und Bioanorganik. Nachrichten Aus Der Chemie, 2016, 64, 232-245.	0.0	0
108	Bimetallic nickel complexes for selective CO ₂ carbon capture and sequestration. Dalton Transactions, 2016, 45, 904-907.	3.3	21

#	Article	IF	CITATIONS
109	A structural view of synthetic cofactor integration into [FeFe]-hydrogenases. Chemical Science, 2016, 7, 959-968.	7.4	122
110	Controlled Flexible Coordination in Tripodal Iron(II) Phosphane Complexes: Effects on Reactivity. Inorganic Chemistry, 2016, 55, 1183-1191.	4.0	19
111	Modulation of extrasynaptic NMDA receptors by synaptic and tonic zinc. Proceedings of the National Academy of Sciences of the United States of America, 2015, 112, E2705-14.	7.1	109
112	Modulating Sonogashira Cross-Coupling Reactivity in Four-Coordinate Nickel Complexes by Using Geometric Control. European Journal of Inorganic Chemistry, 2015, 2015, 2139-2144.	2.0	22
113	A sterically stabilized Fe ^I –Fe ^I semi-rotated conformation of [FeFe] hydrogenase subsite model. Dalton Transactions, 2015, 44, 1690-1699.	3.3	36
114	Versatile Reactivity of a Solvent-Coordinated Diiron(II) Compound: Synthesis and Dioxygen Reactivity of a Mixed-Valent Fe ^{II} Fe ^{III} Species. Inorganic Chemistry, 2014, 53, 167-181.	4.0	21
115	[FeFe]-Hydrogenase models assembled into vesicular structures. Journal of Liposome Research, 2014, 24, 59-68.	3.3	14
116	A Novel [FeFe] Hydrogenase Model with a (SCH2)2Pâ•O Moiety. Organometallics, 2013, 32, 4523-4530.	2.3	30
117	Detection of Nitric Oxide and Nitroxyl with Benzoresorufin-Based Fluorescent Sensors. Inorganic Chemistry, 2013, 52, 3285-3294.	4.0	79
118	Triptycene-Based, Carboxylate-Bridged Biomimetic Diiron(II) Complexes. European Journal of Inorganic Chemistry, 2013, 2013, 2011-2019.	2.0	4
119	Aging-Associated Enzyme Human Clock-1: Substrate-Mediated Reduction of the Diiron Center for 5-Demethoxyubiquinone Hydroxylation. Biochemistry, 2013, 52, 2236-2244.	2.5	23
120	A Siliconâ€Heteroaromatic System as Photosensitizer for Lightâ€Driven Hydrogen Production by Hydrogenase Mimics. European Journal of Inorganic Chemistry, 2013, 2013, 4466-4472.	2.0	36
121	Biomimetic Assembly of the [FeFe] Hydrogenase: Synthetic Mimics in a Biological Shell. ChemBioChem, 2013, 14, 2237-2238.	2.6	3
122	{1,1′â€ (Dimethylsilylene)bis[methanechalcogenolato]}diiron Complexes [2Fe2E(Si)] (E=S, Se, Te) – [FeFe] Hydrogenase Models. Helvetica Chimica Acta, 2012, 95, 2168-2175.	1.6	15
123	A C2-symmetric, basic Fe(iii) carboxylate complex derived from a novel triptycene-based chelating carboxylate ligand. Dalton Transactions, 2012, 41, 9272.	3.3	7
124	New Approach to [FeFe]â€Hydrogenase Models Using Aromatic Thioketones. European Journal of Inorganic Chemistry, 2012, 2012, 318-326.	2.0	16
125	Influence of the Introduction of Cyanido and Phosphane Ligands in Multifunctionalized (Mercaptomethyl)silane [FeFe] Hydrogenase Model Systems. European Journal of Inorganic Chemistry, 2011, 2011, 581-588.	2.0	21
126	Diiron Dichalcogenolato (Se and Te) Complexes: Models for the Active Site of [FeFe] Hydrogenase. European Journal of Inorganic Chemistry, 2011, 2011, 986-993.	2.0	50

#	Article	IF	CITATIONS
127	Effiziente Aktivierung des Treibhausgases CO2. Angewandte Chemie, 2011, 123, 4350-4352.	2.0	1
128	Efficient Activation of the Greenhouse Gas CO ₂ . Angewandte Chemie - International Edition, 2011, 50, 4262-4264.	13.8	22
129	Hydroxy and ether functionalized dithiolanes: Models for the active site of the [FeFe] hydrogenase. Journal of Organometallic Chemistry, 2011, 696, 1084-1088.	1.8	14
130	Reactions of 7,8â€Dithiabicyclo[4.2.1]nonaâ€2,4â€diene 7â€ <i>exo</i> â€Oxide with Dodecacarbonyl Triiron Fe ₃ (CO) ₁₂ : A Novel Type of Sulfenato Thiolato Diiron Hexacarbonyl Complexes. Chemistry - an Asian Journal, 2010, 5, 1600-1610.	3.3	17
131	Synthetic and Electrochemical Studies of [2Fe2S] Complexes Containing a 4â€Aminoâ€1,2â€dithiolaneâ€4â€carboxylic Acid Moiety. European Journal of Inorganic Chemistry, 2010, 2010, 5079-5086.	2.0	9
132	Models for the Active Site in [FeFe] Hydrogenase with Iron-Bound Ligands Derived from Bis-, Tris-, and Tetrakis(mercaptomethyl)silanes. Inorganic Chemistry, 2010, 49, 10117-10132.	4.0	70
133	Reaction of Fe3(CO)12 with octreotide—chemical, electrochemical and biological investigations. Dalton Transactions, 2010, 39, 3065.	3.3	14
134	Investigation of amino acid containing [FeFe] hydrogenase models concerning pendant base effects. Journal of Inorganic Biochemistry, 2009, 103, 1236-1244.	3.5	18
135	Preparation and Characterization of Homologous Diiron Dithiolato, Diselenato, and Ditellurato Complexes: [FeFe]-Hydrogenase Models. Organometallics, 2009, 28, 6666-6675.	2.3	76
136	Functionalized Sugars as Ligands towards Waterâ€Soluble [Feâ€only] Hydrogenase Models. European Journal of Inorganic Chemistry, 2008, 2008, 5112-5118.	2.0	59
137	Oxidation of Diiron and Triiron Sulfurdithiolato Complexes: Mimics for the Active Site of [FeFe]-Hydrogenase. Chemistry and Biodiversity, 2008, 5, 2023-2041.	2.1	27
138	Synthesis and Characterization of Hydroxyâ€Functionalized Models for the Active Site in Feâ€Onlyâ€Hydrogenases. Chemistry and Biodiversity, 2007, 4, 2138-2148.	2.1	35
139	Role‧pecialized Division of Labor in CO2ÂReduction with Doublyâ€Functionalized Iron Porphyrin Atropisomers. Angewandte Chemie, 0, , .	2.0	1